Molecular Imprinted Graphene Oxide Nanocomposite for Optical Sensing of Nicotine in Human Blood Plasma

Sehrish Qazi, Huma Shaikh*, Ayaz Ali Memon, and Shahabuddin Memon
National Centre of Excellence in Analytical Chemistry, University of Sindh, Jamshoro, 76080, Pakistan.
huma.hashu@gmail.com*

(Received on 17th January 2020, accepted in revised form 13th July 2020)

Summary: Among all psychotropic alkaloids, nicotine is more addictive, carcinogenic and capable of causing many health problems. This work is based on the development of highly robust, cheap, reliable, selective and sensitive nicotine imprinted graphene oxide nanocomposite (ImpGO nanocomposite) based optical sensor for determination of nicotine in human plasma. The ImpGO nanocomposite has been thoroughly characterized using different techniques i.e. FT-IR, SEM, TEM, Raman, etc. These characterizations revealed that ImpGO nanocomposite is comprised of single layer of graphene oxide successfully modified with imprinted polymer. The synthesized material was utilized to selectively determine nicotine using UV-vis spectrophotometer in BR buffer of 0.1 M at pH 3 and diluted human plasma. The effect of parameters such as buffer concentration, pH, amount of nanocomposite, etc on determination of nicotine using ImpGO nanocomposite were studied thoroughly. Thus, a sensitive optical method was developed for determination of nicotine in human plasma with linear range of 22-370 pM along with LOD and LOQ of 7 pM and 22 pM, respectively. The selectivity of sensor was evaluated using homologues of nicotine such as nicotine amide, caffeine and cotinine. The results obtained from biological samples showed that developed optical sensor is efficient in complex matrices of real sample.

Key words: Graphene oxide, Imprinting, Nanocomposite, Nicotine, Selectivity, Optical sensing.

Introduction

Nicotine, 3-(1-methyl-2-pyrrolidinyl) pyridine is a hygroscopic oily liquid present in the leaves of *Nicotiana tabacum*. It is one of the highly toxic chemicals belonging to the tobacco alkaloids [1]. A tobacco plant contains 5 percent nicotine by weight. Cigarettes contain 8 to 20 milligrams (mg) of nicotine (depending on the brand), but only approximately 1 mg is absorbed in the human body. The deep inhalation of cigarette smoke carries nicotine to the central nervous system within 20s. Nicotine affects nicotinic cholinergic receptors and most organ systems in the body because it is one of the highly addictive drugs [2]. The prominent symptoms of exposure to nicotine are bronchitis, emphysema, cyanosis, etc. Therefore, excessive smoking causes lung cancer, bladder cancer, and cancer of the larynx and esophagus [3]. Nicotine also effects appetite and food intake [4]. The above mentioned drawbacks urge to determine trace level of nicotine using highly selective analytical methods. The analytical methods based on sensing phenomenon are replacing conventional analytical methods based on tedious extraction protocols and expensive instruments. This is due to the high selectivity and sensitivity of sensing materials that are the heart of sensor. The selectivity of graphene based optical sensors can be enhanced efficiently by making composites with molecular imprinted polymers. Molecularly imprinted polymers are synthesized in the presence of template molecule by using molecular imprinting technique, after the removal of template, the specific binding sites with same shape, size and orientation of functionalities are left into the polymeric matrix. These imprinted binding sites have an affinity for the template molecule over other structural related compounds [5]. MIPs offer several advantages such as high selectivity, recognition properties, reproducibility robustness, stability, low cost, and ease of scale preparation which are very useful for the development of high performance sensor [6, 7]. The graphene oxide (GO) based molecularly imprinted polymers exhibit excellent affinity and selectivity for target molecule. Like graphene, graphene oxide has high rebinding capacity, large surface area that helps in complete removal of templates. The accessibility and kinetics of target molecules have been improved by graphene oxide due to large surface area which helps template molecule to be on its surface. The combination of GO and molecularly imprinted polymers leads to greater sensitivity and affinity for detection of molecule of interest [8] because sensitivity of detection of an imprinted sensor depends on specific imprinted sites on the surface of the sensor and use of composite materials [5]. Moreover, imprinted GO composite materials in sensors have received increased attention because of their remarkable properties, large surface area, ultra fast response time, excellent biocompatibility, high surface to volume ratio, broad band light absorption, ability to quench florescence, outstanding robustness and flexibility [9]. They are material with stability, high mechanical strength and fascinating electronic and optical properties. Graphene oxide is considered to

*To whom all correspondence should be addressed.

enhance nano electronics for swift optical communications due to its excellent optical behaviors [10]. These properties of graphene oxide are excellent for using them as detection material and can also give very sensitive Uv-based methods; though Uv-visible spectrophotometer is non-sensitive technique and methods based on it have high detection and quantification limits. However, graphene oxide based composites can perform as sensitive optical sensors very well even for Uv-visible spectrophotometer. Wang *et al*. [11] have developed visible light photoelectrochemical sensor for the detection of 4-aminophenol. The developed sensor was based on MIP/CdS-GR/FTO modified electrode. The photoelectrochemical response was linear in the range of 5.0×10^{-8} mol/L to 3.5×10^{-6} mol/L and detection limit was found to be 2.3×10^{-8} mol L^{-1}. Li *et al.* [12] have developed sensor for electrochemical detection of dibutyl phthalate. The developed sensor was based on (MGO@AuNPs-MIPs). The response was linear in the range from 2.5×10^{-9} to 5.0×10^{-6} mol/L with a detection limit of 8.0×10^{-10} mol/L. Zeng *et al*. [13] have also developed sensor for electrochemical detection of 4-nitorophenol. The proposed sensor was comprised of rGO and MIP composites. The sensor response was linear from 0.001 to 100.0 µM with limit of detection of 0.005 µM. Cui *et al*. [14] have reported molecularly imprinted sensor based on PtAu-GrCNTs composite for the detection of propyl gallate. Under optimal condition the senor response was linear from 7×10^{-8} to 1×10^{-5} mol L^{-1} of propyl gallate with limit of detection of 2.51×10^{-8} mol L^{-1}. Luo *et al*. [15] have developed electrochemical sensor for the detection of 4-nitrophenol. The developed sensor was based on GR/MIPs composite. The response of sensor was linear in range 0.01 to 100 µM with a limit of detection 5 nM. Yao *et al.* [16] have devised SPR sensor for the detection of ractopamine. The developed sensor was comprised of MIP/GNPs/rGO composite. The sensor response was linear from 20 ng/mL to 1000 ng/mL with a detection limit of 5 ng/mL. Bagheri *et al*. [17] have proposed sensor for electrochemical detection of nitrite and nitrate. The developed sensor is based on (Cu/MWCNT/RGO). The sensor response was linear from 0.1 µM to 75 µM with detection limits 30 nM and 20 nM. More recently, Zhang *et al.* [18] prepared sensor based on CdTe@[emim]MP-amimRG nanocomposite for electrochemical detection of puerarin. Similarly, Gao *et al*. [19] developed sensor comprised of HAP-rGO nanocomposite for electrochemical detection of hydrazine. The sensor responded linear in the range of 2.5 µM to 0.26 mM with a limit of detection of 0.43 µM. Er *et al*. [20] synthesized sensor based on PtNPs@GRP/NFN/GCE nanocomposite for electrochemical detection of Silodosin. The sensor response was linear from 1.8 nM to 290.0 nM with limit of detection 0.55 nM. Thus, most of the recently reported sensors based on graphene or graphene oxide nanocomposites are electrochemical sensors with fewer reports of SPR sensors. The SPR based sensing technique is comparatively more expensive among the other optical sensing techniques. Moreover, the reports for sensitive UV-vis spectrophotometer based graphene/ graphene oxide nanocomposites optical sensors are even less.

In this work, we have developed novel Nicotine imprinted graphene oxide nanocomposite (ImpGO nanocomposites) and utilized it for optical sensing based on ultra sensitive Uv-visible spectrophotometric detection of nicotine in human plasma. UV-vis spectrophotometer is relatively cheaper, swift and simple technique as compared to other optical devices. Imprinted graphene oxide composite provided specific binding sites for nicotine. The developed optical sensor exhibited an excellent selectivity and sensitivity for the detection of nicotine down to pM. Based on obtained results, the proposed optical sensor comprised of imprinted graphene oxide composite was effectively used to detect nicotine in human blood plasma.

Experimental

The details of chemicals and reagents is given in the supplementary data under section 2.1.S

The details of instrumentation is also given in the supplementary data under section 2.2.S

Synthesis of nicotine ImpGO nanocomposite

GO was synthesized using graphite flakes by Hummer's method [21]. Synthesized GO was intercalated with thiosalicylic acid (TSA) (10%). Precisely, 4 mL of thiosalicylic (10%) and 20 mg GO were added in a beaker and heated at 80 ºC for 4 hours in hot water bath. Here heating is necessary to unstack and straighten the stacked sheets of GO. Resulting product was then allowed to cool down and washed thoroughly with deionized water to remove excess of TSA. To prepare imprinted nano-composite; first prepolymerization complexation was carried out by dissolving 0.1 M nicotine standard (template) in 16 mL of DI water maintained at pH 3. To this soultion 10 mg of TSA intercalated GO (TSA@GO) was added and mixture was sonicated for 2 hours. Then to this mixture; 2 mL of pyrrole was added and stirred at 95 ºC for 12 hrs. The prepared material was washed by methanol for removal of nicotine. Fig. 1 shows the schematic representation of synthesis procedure for ImpGO nanocomposite.

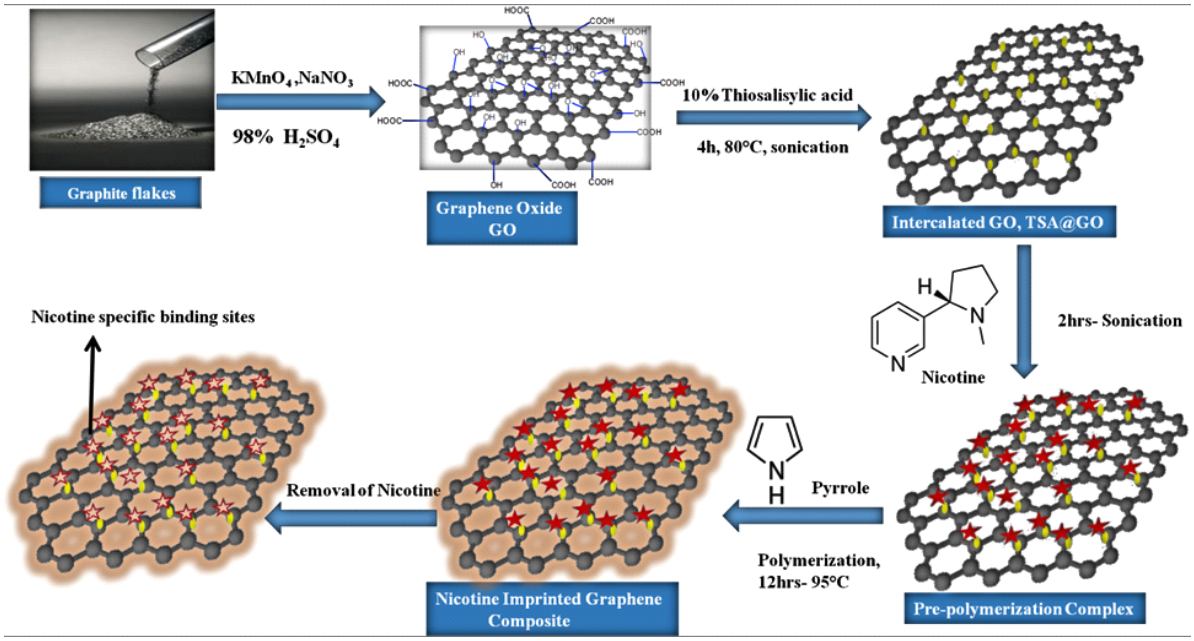

Fig. 1: Schematic representation for the synthesis of Nicotine imprinted GO nanocomposite.

The procedures for optimization of optical parameters for detection of nicotine using ImpGO nanocomposites, evaluation of selectivity of developed sensor and collection and processing of real samples are given in supplementary data under sections 2.3.S, 2.4.S and 2.5.S, respectively.

Result and Discussion

Characterization

The detailed FTIR spectra and their explanation is given in the supplementary data under section 3.1.S

Raman spectroscopy is technique that is often used to study the defects disorders and layers of graphene oxide. There are two main features of Raman spectra that characterize graphene oxide. The G-mode that appears in first order scattering E2g photon of sp^2 carbon atoms appear at higher energy 1575 cm^{-1} while breathing mode within A1g symmetry of j-point arising from D band appearing at lower energy i.e. 1350 cm^{-1}. In Fig 2A which is the raman spectra of GO the G band appears around 1587 cm^{-1} because of the existence of isolated double bonds that vibrate at higher frequencies. Increased prominence in the D band at 1314 cm^{-1} means a decrease in size of the sp^2 domain due to increased oxidation [22]. In Fig 2B, TSA@GO also exhibits the G band appearing around 1584 cm^{-1} while D band appears around 1334 cm^{-1}. The G band is sensitive to number of graphene layers. In (Fig 2A) GO the G band appears around 1587 cm^{-1} shows that single layer of graphene is present whereas in (Fig 2B) TSA@GO after intercalation G band appears at around 1584 cm^{-1} shows layer thickness increases i.e. bilayer of graphene oxide is present [23]. The D band is also known as disorder or defect band and its intensity indicates the level of defect in graphene oxide. Conversely, in TSA@GO after intercalation its intensity decreased which indicates that the defect has been reduced. In (Fig 2B) the D/G intensity ratio for TSA@GO is 1.1 which is lower than GO i.e. 1.4 indicates that TSA has been intercalated with GO [24]. In (Fig 2C) the G band at 1658 cm^{-1} comes from polypyrrole this peak combined with G band to give broad G band [25]. Conversely, the D/G ratio decreases to 0.5 because of decrease in disorder of synthesized material. 2D peak is important in the Raman spectroscopy. Its position and shape are used to predict number of graphene oxide layers. 2D peak is appearing lower than 2700 cm^{-1} indicating the presence of single layer of graphene oxide. If it appears at 2700 cm^{-1}, then the bilayer graphene oxide is present. In (Fig 2C) ImpGO nanocomposite the 2D peak at around 2099 cm^{-1} indicates that single layer of graphene is present in this composite [26].

SEM study is used to investigate the surface morphology of ImpGO nanocomposite. In (Fig 3A) graphite shows stacked sheets. However, the surface morphology of GO has been changed as shown in (Fig 3B) [27]. In comparison to GO, TSA@GO (Fig 3C) exhibits a curved thin flaky appearance. In (Fig 3D) ImpGO nanocomposite shows a dense and quite rough surface, indicating that imprinted polypyrrole has aligned on the surface of ImpGO nanocomposite [15].

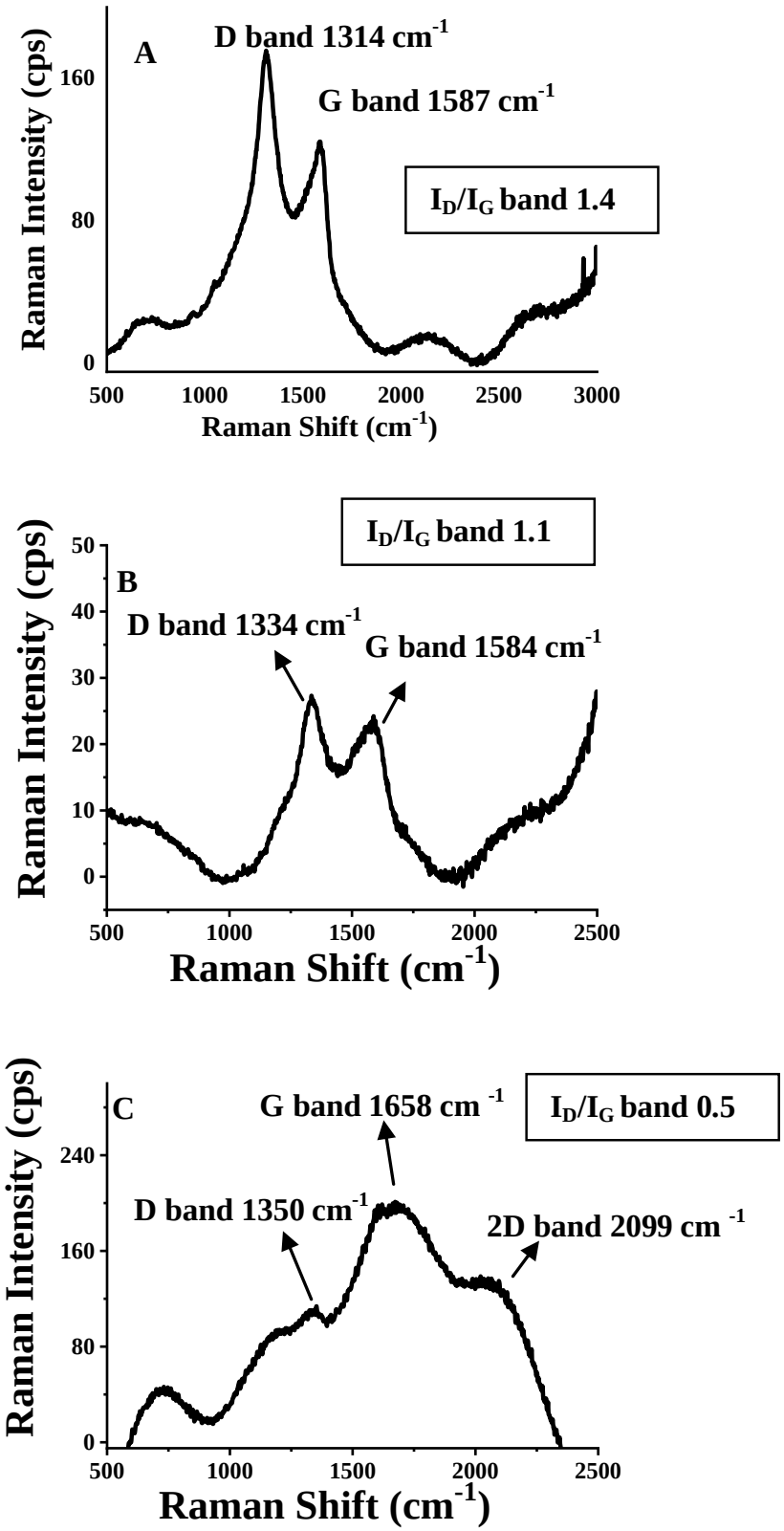

Fig. 2: Raman spectra of (A) GO, (B) TSA@GO, (C) ImpGO nanocomposite.

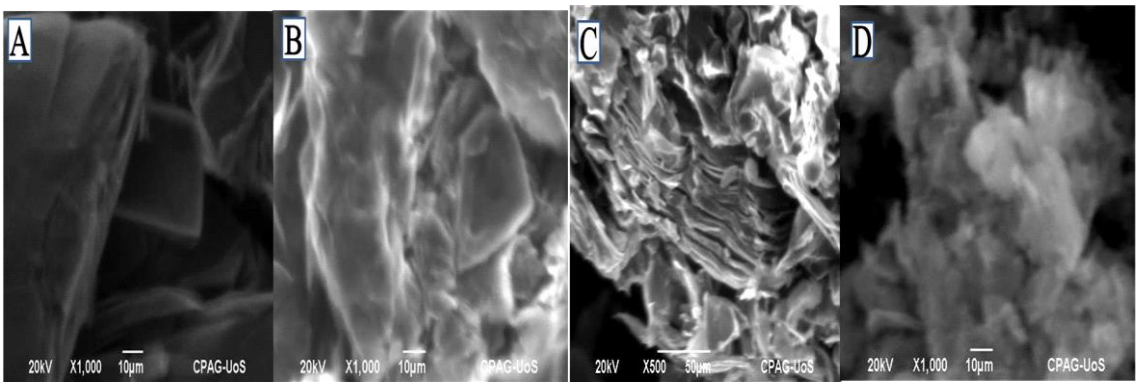

Fig 3: SEM image of (A) Graphite, (B) GO, (C) TSA@GO, (D) ImpGO nanocomposite.

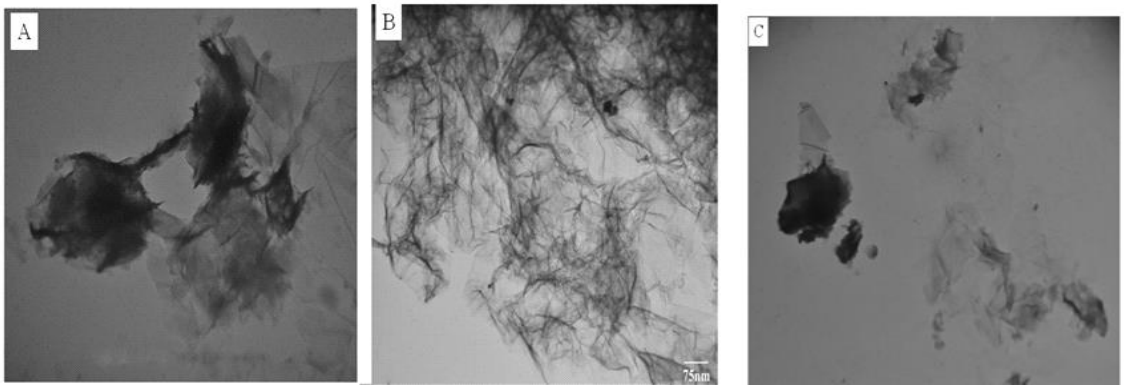

Fig. 4: TEM image of (A) GO, (B) TSA@GO, (C) ImpGO nanocomposite.

The morphological structure of prepared material was also examined by TEM. In Fig 4A, the wrinkles on GO show sheet like morphology is preserved while the darker portion shows more graphene sheets [28]. While in (Fig 4B) TSA@GO wrinkles are retained even after intercalation but the number of stacked sheets has been reduced after intercalation [24]. Whereas, the (Fig 4C) TEM image of ImpGO nanocomposite shows that one sheet is being aligned with the nicotine imprinted polypyrrole. However, wrinkles are still there and sheet is uniformly distributed with nicotine imprinted polypyrrole [29].

Interaction of ImpGO nanocomposite with nicotine

Fig 5 shows Uv-visible spectra of ImpGO nanocomposite in the presence of nicotine (22 pM) and ImpGO nanocomposite alone in water. It is clearly seen that ImpGO nanocomposite does not show any absorption around 295 nm. However, when minute concentration of nicotine is added a band appeared at 295 nm due to the presence of nicotine. Moreover, the characteristic peak of nicotine around 260 nm shifted to 295 nm which is a red shift occurred due the interaction of ImpGO nanocomposites with nicotine. Uv-vis spectrophotometer cannot detect such low concentration of nicotine in the absence of sensing material; it is due to the incorporation of graphene oxide and MIP which resulted in composite material that provides a sensitivity enhancement by inducing large field enhancement at the substrate interface [30]. Furthermore, imprinting is also playing its role in selectivity of sensing material as ImpGO nanocomposite contains imprinted binding sites which recognize the nicotine selectively and get activated.

Optimization of sensing conditions for nicotine using ImpGO nanocomposite

Optimization of amount of ImpGO nanocomposite

To optimize the amount of ImpGO nanocomposite for maximum response of nicotine, the standard solution of nicotine (7 pM) was spiked with different amounts of ImpGO nanocomposite. As observed in (Fig 3S) when the amount of ImpGO nanocomposite increases from 10 µg to 220 µg in 7 pM of nicotine the response greatly enhances till 200 µg of ImpGO nanocomposites, however, slight increments occur with further increase of the ImpGO nanocomposite. Thus, 200 µg of ImpGO nanocomposite was selected for further studies [31]. The Uv-visible

spectra of effect of amount of ImpGO nanocomposite for the maximum response of nicotine is given in the supplementary data in Fig 3.S.

Optimization of pH and buffer concentration

The pH was investigated using 0.1 M Britton-Robinson Buffer in the range of pH 2 to12 and response of 7 pM of nicotine was checked on ImpGO nanocomposite. It was observed that (Fig 6) at 295 nm ImpGO nanocomposite showed maximum response with BR buffer of pH 3. The maximum intensity and exact position of peak depends upon nature of solvent, analyte and sensing material [32]. Depending on pH the nicotine may be found in one of three types such as mono protonated, diprotonated and unprotonated [33]. It is mono protonated at pH less than 3, diprotonated at pH 3 to 8 and unprotonated at pH greater than 8, respectively [34]. Nicotine is basic compound having two pKa values of 8.02 and 3.12 and having capability to form hydrogen bonds [35]. Thus, keeping this in mind the pre-polymerization complexation of nicotine with TSA@GO was carried out at pH 3. Therefore, it interacts with ImpGO nanocomposite through hydrogen bonds at pH 3 as the active binding sites are selective to diprotonated nicotine. However, the absorption band shifts from 260 nm to 295 nm due to interaction of nicotine with ImpGO [36]. Therefore, BR buffer at pH 3 was selected for further studies.

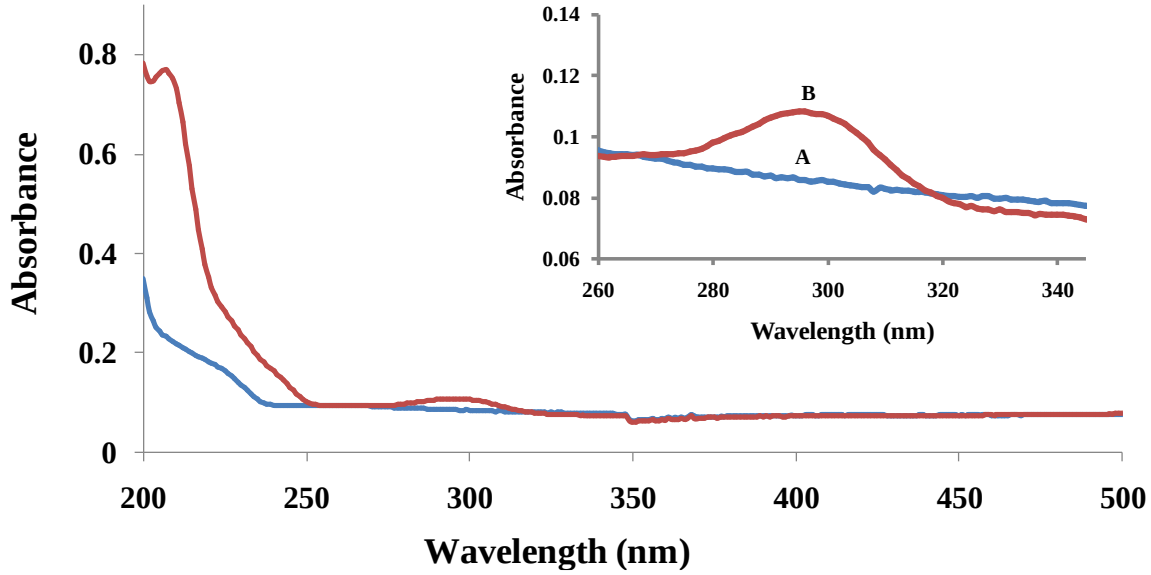

Fig 5: The Uv-visible spectra of interaction; Insight (A) ImpGO nanocomposite, (B) ImpGO nanocomposite with nicotine.

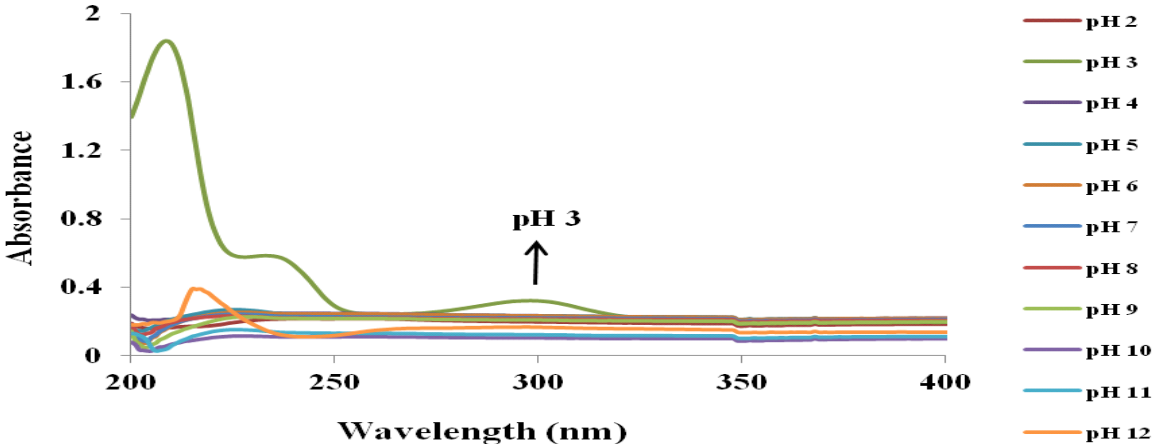

Fig. 6: Effect of BR buffer at different pH on sensing efficiency of ImpGO nanocomposite for nicotine.

Fig 4.S in supplementary data shows the influence of buffer concentration on sensing ability of ImpGO nanocomposite for nicotine. The BR buffer of pH 3 was evaluated in the concentration range of 0.005 to 0.5 M. It is clearly seen that with the increase in concentration of BR buffer the response of ImpGO nanocomposite linearly increases till 0.1 M (peak at 295 nm) due to the interaction of nicotine with the ImpGO nanocomposite. Conversely, further increase in concentration of BR buffer decreased the response. This may be due to the influence of higher concentration of buffer components that inactivate the binding sites. Therefore 0.1M BR buffer of pH 3 was selected for further studies.

Table-1: Analytical Figs of merit for determination of nicotine using ImpGO nanocomposite in human plasma

Analytical Figs of Merit	
Linear Range (pM)	**22-370**
Linearity (r^2)	**0.999**
Slope (a)	**0.00026**
Intercept (b)	**0.24**
LOD (pM)	**7**
LOQ (pM)	**22**
Intra-assay Precision (RSD %)	
22 pM (n=3)	**0.86 %**
155 pM (n=3)	**0.74 %**
370 pM (n=3)	**0.16 %**
Inter-assay Precision (RSD %)	
22 pM (n=3, 3days)	**0.76 %**
155 pM (n=3, 3days)	**0.68 %**
370 pM (n=3, 3days)	**0.14 %**

Method validation using ImpGO nanocomposite in human blood plasma

In order to check the effect of complex matrices on the performance of ImpGO nanocomposite, a method was also developed and validated in blood plasma using ImpGO nanocomposite. The human blood plasma was processed, spiked with different concentrations of nicotine and diluted with 0.1 M BR buffer as described in section 2.4S in supplementary data. The Table-1 shows the analytical Figs of merit for determination of nicotine in blood plasma. In this method the linear range was obtained from 22 to 370 pM with the linearity 0.999 whereas the limit of detection 7 pM and limit of quantification 22 pM were obtained with acceptable RSD values of intraday and interday precision (Fig 7). The results clearly show that the efficiency of ImpGO nanocomposite is not compromised even in complex matrices. However, the absorption peak of nicotine is observed at around 275 nm. This shift of absorption band from 295 nm (BR Buffer) to 275 nm (diluted plasma) in the presence of ImpGO composites is due to the matrix effect. The excellent LOD and LOQ values show that in spite of complex matrix the selectivity and sensitivity of sensing material is not compromised. The sensitivity and specificity of ImpGO nanocomposite for nicotine in blood plasma is almost same as it was in the standard solutions of nicotine.

Interference study

The imprinting factor is used to determine the selectivity of prepared imprinted material; it shows the strength of interaction of template and functional monomer. If the imprinting factor value is greater, it indicates that there is strong interaction between template and functional monomer. If the imprinting factor value is smaller, it indicates that there is weak interaction between template and functional monomer [37]. The imprinting factor of nicotine imprinted graphene oxide nanocomposite was checked with the homologues of nicotine such as nicotinamide, caffeine and cotinine in human plasma. The imprinting factor was calculated using following equation by taking the absorbance of nicotine and its homologues having same concentration, using imprinted and non-imprinted graphene oxide nanocomposite.

$$Coefficient\ of\ selectivity\ (k) = (Abs\ (template))/(Abs\ (competitor)$$

$$Relative\ Selectivity\ Coefficient\ (k') = \frac{k\ (ImpGO\ nanocomposite)}{k(NImpGO\ nanocomposite)}$$

The selectivity study (Table-2) revealed that nicotine imprinted graphene oxide nanocomposite is 2.4 times more selective for nicotine than nicotinamide and 1.6 times more selective for nicotine than caffeine and 1.1 times more selective for nicotine than cotinine due to specific binding sites that recognize the target molecule.

Recovery study

The developed method was applied on real samples such as blood plasma of smokers. In this regard the three different concentration of nicotine were spiked in blood plasma of smokers along with ImpGO nanocomposite. The Table-3 shows the recoveries % obtained from blood plasma of smokers. In all samples, there is negligible matrix effect as the prepared material is more selective and sensitive for nicotine.

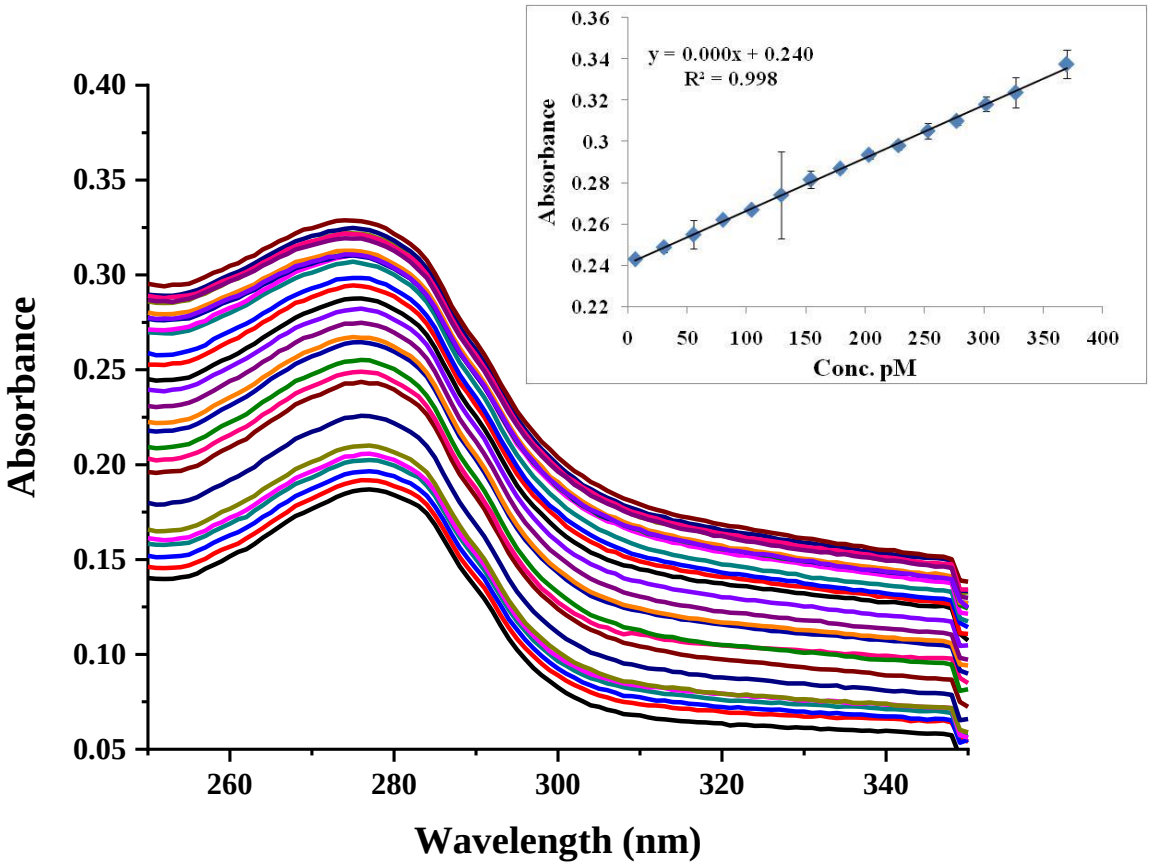

Fig. 7: Calibration curve obtained for different concentration of nicotine using ImpGO nanocomposite in blood plasma.

Table-2: Selectivity and relative selective coefficient of ImpGO nanocomposite.

Alkaloids	ImpGO nanocomposite	NImpGO nanocomposite	k ImpGO nanocomposite	k NImpGO nanocomposite	k'
Nicotine	0.34	0.14			
Nicotine amide	0.09	0.09	3.7	1.5	2.4
Caffeine	0.12	0.08	2.8	1.75	1.6
Cotinine	0.18	0.08	1.9	1.7	1.1

Table-3: Recovery % of spiked human plasma using ImpGO nanocomposite for nicotine.

Conc.(p)	Recovery %									
Nicotine	Plasma 1	Conc. Found	Plasma 2	Conc. Found	Plasma 3	Conc. Found	Plasma 4	Conc. Found	Plasma 5	Conc. Found
22	90	19.8	92	20.24	94	20.68	105	23.1	102	22.44
155	93	144.15	93	144.15	96	148.8	108	167.4	103	159.65
370	97	358.9	98	362.6	99	366.3	110	407	105	388.5

Conclusion

A new optically active nicotine imprinted graphene oxide nanocomposite was prepared. The nanocomposite was utilized for selective optical sensing of nicotine in human blood plasma. The calibration curve for nicotine determination was obtained at optimized conditions using human blood plasma diluted with 0.1 M BR buffer at pH 3. Linear range and limit of detection at ultra trace levels of nicotine (pM) were obtained. Furthermore, short analysis time, good selectivity and accuracy, low cost and simple preparation process are among the advantages of the proposed sensor. The proposed nanocomposite is excellent for sensing of nicotine in biological samples.

Conflict of interest

All the authors of this manuscript declare that there are no conflicts of interest to declare for the research data presented in this manuscript.

References

1. S. Al-Tamrah, Spectrophotometric determination of nicotine , *Anal Chim Acta* **379**, 75 (1999).
2. L. Vlase, L. Filip, I. Mindrutau, and S. Leucuta, Determination of nicotine from tobacco by LC–MS–M,*Stud. Univ. Babeş-Bolyai, Phys***4,** 19 (2005).
3. S. M. Attaf and H. A. Omara, Spectrophotometric determination of nicotine in Cigarette tobacco and biological samples of smokers, *World J Pharm Pharm Sci* **1327**, 1340 (2014).
4. Y. H. Jo, D. A. Talmage, and L. W. Role, Nicotinic receptor-mediated effects on appetite and food intake, *J Neurobiol***53**, 618 (2002).
5. B. B. Prasad, A. Kumar, and R. Singh, Synthesis of novel monomeric graphene quantum dots and corresponding nanocomposite with molecularly imprinted polymer for electrochemical detection of an anticancerous ifosfamide drug, *Biosens Bioelectron***94**, 1 (2017).
6. G. Wulff, Fourty years of molecular imprinting in synthetic polymers: origin, features and perspectives,*Microchim Acta*, **180**, 1359 (2013).
7. L. Ye and K. Mosbach, Molecular imprinting: synthetic materials as substitutes for biological antibodies and receptors,*Chem Mater* **20**, 859 (2008).
8. S. Alexander, P. Baraneedharan, S. Balasubrahmanyan, and S. Ramaprabhu, Modified graphene based molecular imprinted polymer for electrochemical non-enzymatic cholesterol biosensor, *Eur Polym J***86**, 106 (2017).
9. B. N. Shivananju, W. Yu, Y. Liu, Y. Zhang, B. Lin, S. Li, and Q. Bao, The Roadmap of Graphene-Based Optical Biochemical Sensors,*Adv Funct Mater***27**, 1603918 (2017).
10. K. W. C. Lai, N. Xi, H. Chen, C. K. M. Fung, and L. Chen, *Development of graphene-based optical detectors for infrared sensing applications, Ieee Sens J*, **398**-401(IEEE, 2011)
11. R. Wang, K. Yan, F. Wang, and J. Zhang,A highly sensitive photoelectrochemical sensor for 4-aminophenol based on CdS-graphene nanocomposites and molecularly imprinted polypyrrole, *Electrochim Acta***121,** 102 (2014).
12. X. Li, X. Wang, L. Li, H. Duan, and C. Luo, Electrochemical sensor based on magnetic graphene oxide@ gold nanoparticles-molecular imprinted polymers for determination of dibutyl phthalate, *Talanta***131**, 354 (2015).
13. Y. Zeng, Y. Zhou, T. Zhou, and G. Shi, A novel composite of reduced graphene oxide and molecularly imprinted polymer for electrochemical sensing 4-nitrophenol, *Electrochim Acta*130, 504 (2014).
14. M. Cui, J. Huang, Y. Wang, Y. Wu, and X. Luo, Molecularly imprinted electrochemical sensor for propyl gallate based on PtAu bimetallic nanoparticles modified graphene–carbon nanotube composites, *Biosens Bioelectron* **68**, 563 (2015).
15. J. Luo, J. Cong, J. Liu, Y. Gao, and X. Liu, A facile approach for synthesizing molecularly imprinted graphene for ultrasensitive and selective electrochemical detecting 4-nitrophenol,*Anal Chim Acta***864**, 74 (2015).
16. T. Yao, X. Gu, T. Li, J. Li, J. Li, Z. Zhao, J. Wang, Y. Qin, and Y. She, Enhancement of surface plasmon resonance signals using a MIP/GNPs/rGO nano-hybrid film for the rapid detection of ractopamine, *Biosens Bioelectron* **75**, 96 (2016).
17. H. Bagheri, A. Hajian, M. Rezaei, and A. Shirzadmehr, Composite of Cu metal nanoparticles-multiwall carbon nanotubes-reduced graphene oxide as a novel and high performance platform of the electrochemical sensor for simultaneous determination of nitrite and nitrate, *J Hazard Mater***324,** 762 (2017).
18. H. Zhang, Y. Shang, T. Zhang, K. Zhuo, and J. Wang, Engineering graphene/quantum dot interfaces for high performance electrochemical nanocomposites in detecting puerarin, *Sensor Actuat B-Chem* **242**, 492 (2017).
19. F. Gao, Q. Wang, N. Gao, Y. Yang, F. Cai, M. Yamane, F. Gao, and H. Tanaka, Hydroxyapatite/chemically reduced graphene oxide composite: environment-friendly synthesis and high-performance electrochemical sensing for hydrazine, *Biosens Bioelectron* **97**, 238 (2017).
20. E. Er, H. Çelikkan, and N. Erk, An ultra-sensitive 2D electrochemical sensor based on a PtNPs@ graphene/Nafion nanocomposite for determination of α 1-AR antagonist silodosin in human plasma, *Anal Methods-Uk***9**, 3782 (2017).
21. L. Shahriary and A. A. Athawale, Graphene oxide synthesized by using modified hummers approach, *Int J Renew Energy Environ Eng* **2**, 58 (2014).
22. K. N. Kudin, B. Ozbas, H. C. Schniepp, R. K. Prud'Homme, I. A. Aksay, and R. Car,Raman spectra of graphite oxide and functionalized graphene sheets, *Nano Lett***8**, 36 (2008).
23. J. Hodkiewicz, Characterizing graphene with Raman spectroscopy, *Thermo Fisher Scientific*, Application Note: 51946 (2010)Madison, WI, USA.

24. K. Zhang, L. Mao, L. L. Zhang, H. S. O. Chan, X. S. Zhao, and J. Wu, Surfactant-intercalated, chemically reduced graphene oxide for high performance supercapacitor electrodes, *J Mater Chem***21**, 7302 (2011).
25. L. Qu, G. Shi, J. Yuan, G. Han, and F. e. Chen, Preparation of polypyrrole microstructures by direct electrochemical oxidation of pyrrole in an aqueous solution of camphorsulfonic acid, *J Electroanal Chem***561**, 149 (2004).
26. Y. Hernandez, V. Nicolosi, M. Lotya, *et al.*, High-yield production of graphene by liquid-phase exfoliation of graphite, *Nat Nanotechnol***3**, 563 (2008).
27. Y. Zeng, Y. Zhou, L. Kong, T. Zhou, and G. Shi, A novel composite of SiO2-coated graphene oxide and molecularly imprinted polymers for electrochemical sensing dopamine, *Biosens Bioelectron* **45**, 25 (2013).
28. Q. Huamin, F. Lulu, X. Li, L. Li, S. Min, and L. Chuannan, Determination sulfamethoxazole based chemiluminescence and chitosan/graphene oxide-molecularly imprinted polymers, *Carbohyd Polym***92**, 394 (2013).
29. X. M. Feng, R. M. Li, Y. W. Ma, R. F. Chen, N. E. Shi, Q. L. Fan, and W. Huang, One-step electrochemical synthesis of graphene/polyaniline composite film and its applications, *Adv Funct Mater***21**, 2989 (2011).
30. P. O. Patil, G. R. Pandey, A. G. Patil*et al.*, Graphene-based nanocomposites for sensitivity enhancement of surface plasmon resonance sensor for biological and chemical sensing: A review, *Biosens Bioelectron*, **139,** 111324 (2019).
31. H. Xiong, Y. Zhao, P. Liu, X. Zhang, and S. Wang, Electrochemical properties and the determination of nicotine at a multi-walled carbon nanotubes modified glassy carbon electrode, *Microchim Acta***168**, 31 (2010).
32. C. Willits, M. L. Swain, J. Connelly, and B. Brice, *Spectrophotometric determination of nicotine,Anal Chem***22**, 430 (1950).
33. G. H. Lu and S. Ralapati, Application of high-performance capillary electrophoresis to the quantitative analysis of nicotine and profiling of other alkaloids in ATF-regulated tobacco products, *Electrophoresis***19**, 19 (1998).
34. Z. Wu, X. Zhang, Y. Yang, G. Shen, and R. Yu, A sensitive nicotine sensor based on molecularly imprinted electropolymer of o-aminophenol, *Front Chem* In China **1**, 183 (2006).
35. W. M. Mullett, E. P. Lai, and B. Sellergren, Determination of nicotine in tobacco by molecularly imprinted solid phase extraction with differential pulsed elution, *Anal Commun***36**, 217 (1999).
36. J. L. Murray, Honors Thesis, *Nicotine and what else?: HPLC elution optimization for the analysis of alkaloids found in electronic cigarettes*, University of Tennessee at Chattanooga (2014).
37. C. Nantasenamat, T. Naenna, C. I. N. Ayudhya, and V. Prachayasittikul, Quantitative prediction of imprinting factor of molecularly imprinted polymers by artificial neural network, *J Comput Aid Mol Des***19**, 509 (2005).